

RESEARCH PAPER

Sustainable Fabrication of Indium Oxide Nano Thin Film by Tuning Wettability and Rheological Behavior of Inkjet Inks

Zohreh Karami¹, Atasheh Soleimani-Gorgani^{1*}, G. Reza Vakili-Nezhaad²

¹ Department of Printing Science and Technology, Institute for Color Science and Technology, PO Box 16765654, Tehran, Iran

² Department of Petroleum and Chemical Engineering, College of Engineering, Sultan Qaboos University, 33, Muscat 123, Oman

ARTICLE INFO

Article History:

Received 06 April 2024

Accepted 24 June 2024

Published 01 July 2024

Keywords:

Indium oxide

Inkjet Printing

Nano thin-film

Water-based inks

ABSTRACT

Inkjet printing is an alternative, sustainable, cost-effective method for fabricating and depositing thin films. This research uses indium oxide nano-thin films as the transparent conducting electrode (TCE) fabricated by an eco-friendly inkjet printing method. Various indium acetate water-based inks as metal salt precursors were formulated in the first stage. Different co-solvents were used to adjust ink solutions' viscosity and surface tension to improve wettability and optimize the rheological conditions to avoid nozzle clogging of the printers' heads. Plasma pretreatment also increased the hydrophilicity and wettability of the glass substrate to achieve smooth and homogenous printed film. Finally, after enhancing the integrity of the printed film by improving adhesion and wettability, the optimum ink formulation is printed on the plasma treated glass and then subjected to the required thermal treatment process to obtain indium oxide nano-thin film. Complete characterization of the printed indium oxide thin film was carried out through different techniques, including Field Emission Scanning Electron Microscopy (FE-SEM), X-ray Diffraction (XRD), UV/Visible Spectrometry, Photoluminescence (PL) Spectrometry, and Raman Spectrometry towards finding the structures and optical properties of the printed thin film. The uniform and smooth nano-films of indium oxide are deposited on the glass substrate through an eco-friendly and sustainable method.

How to cite this article

Karami Z., Soleimani-Gorgani A., Vakili-Nezhaad G. Sustainable Fabrication of Indium Oxide Nano Thin Film by Tuning Wettability and Rheological Behavior of Inkjet Inks J Nanostruct, 2024; 14(3):917-931. DOI: 10.22052/JNS.2024.03.020

INTRODUCTION

Transparent conductive electrodes (TCE)s are essential for optoelectronic devices such as solar cells, light-emitting diodes, energy-conserving windows, and touch screens. TCEs pass the light through optoelectronic devices with minimum absorption or reflection [1]. Among TCE materials, metal oxides provide better conditions for optoelectronic devices because of their intrinsic

properties [2]. Indium acetate, a water-soluble source of indium, is used in this research as a metal oxide precursor in the deposition of indium tin oxide films.

There are various methods to deposit TCE materials. Inkjet printing is an alternative method to fabricate thin films from functional materials. Unlike other methods used to deposit TCEs, inkjet printing is cost-effective, fast, simple, safe, and

* Corresponding Author Email: asoleimani@icrc.ac.ir



environmentally friendly. The desired pattern is provided on the selected substrate by inkjet printing during a non-contact process without obstacles like masks or vast and expensive equipment types [3]. This method is compatible with a wide variety of TCE materials like metal oxides and reduces material waste.

Indium acetate precursor is used to fabricate indium oxide (IO) nano thin film by inkjet printing deposition method, as the metal acetate salts could be dissolved in water to produce sustainable and environmentally friendly aqueous ink solutions. After printing, the metal oxide nano-thin films provide during the thermal treatment process. The acetates have low decomposition temperatures in the thermal treatment process, which could achieve metal oxide films in lower temperatures.

Formulating an appropriate inkjet ink for commercial DOD (Drop-on-Demand) inkjet printer from the indium acetate solution is the most critical step in inkjet printing of TCE materials. Any cracks, heterogeneity, or non-levelness of printed films regarding the mal functionality of optoelectronic devices. Co-solvents were applied to tuning wettability and rheology behavior of formulated indium acetate inkjet inks to attain high-quality printed films.

Wettability has a crucial role in optimizing the inkjet inks formulations. Wettability and spreading of ink droplets on the substrate influence the adhesion of the printed layer to the substrate [4,5]. The wettability of inks could be investigated by measuring the contact angle of printed droplets and the surface tension of ink solutions [6]. Contact angle analysis notifies about substrate-surface interactions and allows to evaluate of the ink droplets spreading and absorption by analyzing the drop dimensions and contact angles by passing the time.

The rheology behavior of the ink solution is another essential factor that influences the spreading dynamic of the droplet. For inkjet printing, Newtonian low viscosity ink solutions are recommended. Ink solutions behave as Newtonian fluids as the viscosity is constant by varying shear rates [7].

Substrate pretreatment is another way to improve the wettability and adhesion of the printed layer. Glass substrate is a common choice in printing TCE materials, as it is transparent to pass the light from both sides. Inkjet printing of TCE materials

on the glass substrate without any pretreatment leads to the random position of printed materials and non-homogeneity of the printed layer. Several approaches to pretreat the glass substrate include surface washing with Piranha solution and plasma pretreatment. Plasma pretreatment is effective and environmentally friendly, improving the glass surface's hydrophilicity. As a result, the surface energy increases, allowing ink droplets wet the surface better.

Finally, the nano-IO thin film's optical, electrical, and structural properties were investigated and confirmed the high-quality characteristics of the synthesized nano-films.

MATERIALS AND METHODS

Materials

Indium (III) acetate, $\text{In}(\text{C}_2\text{H}_3\text{O}_2)_3$ with 99.99% purity purchased from Sigma-Aldrich Chemical Corporation, Germany. The various co-solvents such as ethylene glycol (EG), diethylene glycol (DEG), triethylene glycol (TEG), tetraethylene glycol (Tetra EG), polyethylene glycol 200 (PEG200), glycerol, and all other chemicals used in this work were laboratory-grade chemicals purchased by Merck Company, UK.

Equipment and instrumentation

The pH, surface tension, and viscosity of the water-based inks were evaluated using 827 pH Metrohm meters (Herisau/Switzerland), Tensiometer K100MK2 (Hamburg, Germany), and Brookfield DVII (New Jersey, USA), respectively. The static and dynamic contact angle of ink solution with the glass substrate and the surface energy of the glass substrate is based on the sessile drop method at 20 °C temperature measured using the optical contact angle measuring device OCA200 (Data physics company, Germany). This device has a CCD camera with a resolution of 768×576 pixels, capable of capturing 50 images per second and analyzing the shape of the drop. An Epson Stylus Photo P50 printer printed the prepared precursor ink inkjet. The inkjet-printed glass slides were dried and heat-treated in an Azar 1250 furnace.

The crystallinity of the IO thin film was examined using high-resolution Grazing incidence X-ray diffraction (GIXRD) on a Philips PW 1730 diffractometer (Netherlands) equipped with $\text{Cu-K}\alpha$ radiation (40kV, 30 mA) in the 2θ range from 20 to 60° with the step of 0.05°. The printed film surface morphology was analyzed by field emission

scanning electron microscope (FE-SEM), model MIRA3 TESCAN-XMU (Czech Republic). Optical transmittance of IO thin film was measured, within the wavelength range of 300–800nm, by a UV/Visible spectrometer (Agilent 8453, Australia). Photoluminescence (PL) was measured on a luminescence spectrometer (Perkin Elmer LS 55, USA). Raman spectra were recorded in the range of 100-2500cm⁻¹ using an (XploRA Plus confocal RAMAN microscope, France SAS) through 532 nm excitation wavelength.

Preparation of indium acetate ink solutions with various co-solvents and complexing agents to achieve optimal formulation

Fluid ink solutions consist of indium acetate salt as a precursor. Initially, indium acetate was dissolved in deionized water as a diluent, then weak organic acid (acetic acid) was added to ink formulation as a complexing agent that improves the solubility of indium acetate in water. Glycol ethers were used as a co-solvent to reduce the rate of water evaporation, prevent the ink from drying out in the nozzle and improve the drying process of the printed droplet. Isopropyl alcohol was

added to the ink formulation to adjust the surface tension so that the ink could jet from the nozzle optimally. Finally, ammonia was added to increase the pH value. Different inks were formulated that were the same in the concentration of indium acetate, isopropyl alcohol, water, and ammonia but were modified by various glycol ethers as co-solvents and weak organic acids as complexing agents and investigate their effect on surface tension and contact angle of formulated inks and its rheological behavior. Finally, all the inks were stirred in ultrasonic for 10 minutes and then filtered through a 0.45 μm diameter syringe filter and a 0.2 μm diameter syringe filter. The formulated inks were printed on glass substrates by the Epson P50 printer.

Various glycol ethers were different in chemical structure, molecular weight, dipole moment, and boiling point used in the indium acetate ink's formulation to investigate the co-solvents' effect. Table 1 shows the formulation of inks 1 to 9 that differ in the type of co-solvent (glycol ether) and complexing agent (weak acid). Table 2 shows the chemical structure of different glycol ethers used in the inks' formulation.

Table 1. Formulation of different inks based on the type of ethylene glycol

Ink (Wt%)	Ink 1	Ink 2	Ink 3	Ink 4	Ink 5	Ink 6	Ink 7	Ink 8	Ink 9
Indium Acetate	2%	2%	2%	2%	2%	2%	2%	2%	2%
Deionized Water	40%	40%	40%	40%	40%	40%	40%	40%	40%
Di Ethylene Glycol Mono Butyl Ether	7%	7%	7%	7%	7%	7%	7%	7%	7%
2-Propanol	1%	1%	1%	1%	1%	1%	1%	1%	1%
Ammonia 25%	10%	10%	10%	10%	10%	10%	10%	10%	10%
Ethylene Glycol	20%	-	-	-	-	-	-	-	-
Di Ethylene Glycol	-	20%	-	-	-	-	-	-	-
Tri Ethylene Glycol	-	-	20%	-	-	-	-	-	-
Tetra Ethylene Glycol	-	-	-	20%	-	-	-	-	-
Poly Ethylene Glycol	-	-	-	-	20%	20%	20%	20%	20%
Formic Acid	-	-	-	-	-	20%	-	-	-
Acetic Acid	20%	20%	20%	20%	20%	-	20%	-	-
Propionic Acid	-	-	-	-	-	-	-	20%	-
Butyric Acid	-	-	-	-	-	-	-	-	20%
pH	6.3	6.3	6.3	6.3	6.3	6.3	6.3	6.3	6.3

Four types of organic acids were used to investigate the effect of a weak acid as a complexing agent: formic acid, acetic acid, propionic acid, and

butyric acid, in which the hydrocarbon chains are increased, respectively. Table 3 shows the chemical structure of complexing agents used in

Table 2. Characteristics of ethylene glycols used in inks formulation

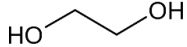
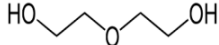
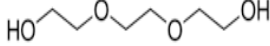
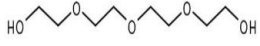
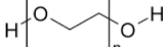
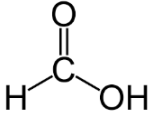
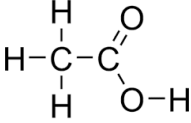
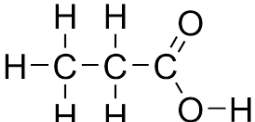
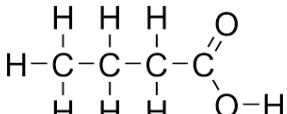
Ink	Co-solvent	Chemical structure	Dipole moment	Boiling point	Vapor pressure (20C)	Density (20C)	Surface tension
1	(EG) Ethylene glycol		2.28	197	0.06	1.115	47.99
2	Diethylene glycol (DEG)		2.69	245	0.002	1.118	48.5
3	Tri ethylene glycol (TRIEG)		2.99	285	0.001>	1.125	45.5
4	Tetra ethylene (Tetra EG) glycol		3.25	329	0.001>	1.126	44.40
5	Polyethylene glycol (PEG)		3.25	300-400	0.001>	1.128	43.5

Table 3. Structure of complexing agents used in inks formulation

Ink	Complexing agent	Boiling point °C	Acid dissociation		Chemical structure of the complexing agent
			constant	pK_a	
6	Formic Acid	100.8	3.77		
7	Acetic Acid	118.1	4.76		
8	Propionic Acid	141	4.82		
9	Butyric Acid	163.5	4.87		

inks formulation.

Indium oxide film preparation and characterization

In this section, the inkjet printing was done after obtaining the optimum ink formulation and the pretreatment of the glass surface. This printer uses a piezoelectric squeeze mode print head that injects ink droplets through a 65 μm nozzle. IO thin films were deposited on microscope glass slides of

20 \times 20 mm by inkjet printing. The ink was ejected from the inkjet printer cartridge and dried at 150°C for 10 minutes; this procedure was repeated three times. Finally, the thermal treatment process was run to achieve IO thin film. The dried film was initially sintered in a furnace heated under the rate of 10°C/min up to 350 °C and held for 3 hours in the air atmosphere. Afterward, the temperature increased up to 550 °C under the same heating rate

Table 4. Viscosity of inks at the highest shear rate

Ink	Viscosity (mPa.s)
1	3.56
2	4.14
3	4.42
4	4.62
5	5.54
6	4.81
7	5.51
8	6.11
9	6.48

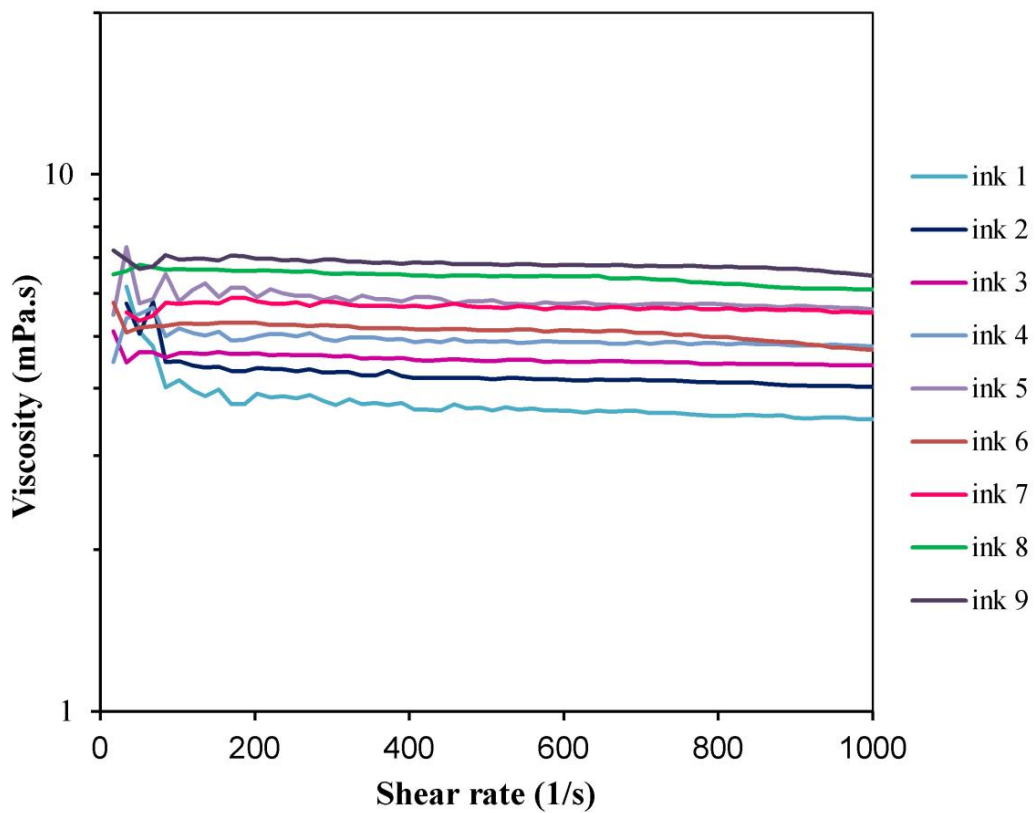


Fig. 1. Rheological Behavior of Inkjet Inks (1-9)

and was maintained at that temperature for 3 h. Then, the samples were cooled down to ambient temperature. Subsequently, the samples were inserted into the glass tube furnace for annealing. The temperature was raised to 350°C at 10°C/min and kept constant for 30 min under the nitrogen atmosphere. Different analyses in the following characterized the prepared IO thin film.

RESULTS AND DISCUSSION

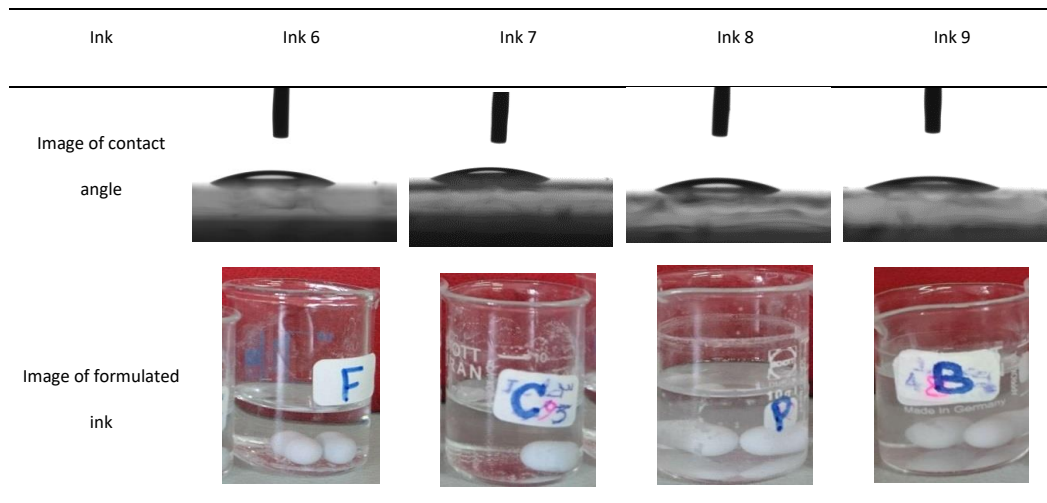
The viscosity of inkjet inks is significant because it affects the ink's rheology behavior when it

passes through the nozzles of the printer head and the performance of the ink during jetting and spreading on the surface. Dissolved nanoparticles' particle size and concentration affect the ink's viscosity. High viscosity ink cannot pass through the nozzles in the printer head, and if the viscosity is too low, the satellite drops form, which ink's droplets come out from the printer's nozzles too much splashing and causing poor print quality [8]. Another important physical property of inkjet ink is surface tension. The surface tension of conductive inks mainly affects the jettability of

Table 5. Surface tension and static contact angle of formulated inks

Sample name	Static CA on glass sample (°)	Surface Tension	Standard Deviation (σ)
Ink 1	32.97	34.35	± 0.01
Ink 2	28.75	34.27	± 0.03
Ink 3	22.01	34.19	± 0.01
Ink 4	22.66	34.10	± 0.02
Ink 5	21.85	33.83	± 0.01
Ink 6	21.56	34.85	± 0.04
Ink 7	21.36	33.79	± 0.01
Ink 8	21.26	33.54	± 0.02
Ink 9	21.06	32.84	± 0.02

Table 6. Image of contact angle of formulated inks



fine droplets from the printers' nozzles and the ink's wetting properties on the substrate in the printing process. The viscosity of DOD inkjet inks should be in the range of 1-25 mPa.s [9], and the recommended range for surface tension is 20-50 $\text{mN}\cdot\text{m}^{-1}$ [10].

Effect of modification of co-solvents and complexing agents on the wettability and rheological behavior of formulated inks

Table 4 indicates the viscosity of the inks (1 to 9) at the highest shear rate (1000 S^{-1}). All inks have viscosity values in the acceptable range for inkjet printing inks. As can be seen, in Ink 1 to Ink 5, the viscosity of the ethylene glycol used in the ink formulation has increased with increasing molecular weight. In Ink 6 to Ink 9, there is a slight difference in the viscosity values of the inks. By changing the type of complexing agent and increasing the hydrocarbon chain of the weak acid used, in other words, by increasing the molecular mass of the complexing agent used in the ink formulation, the viscosity has also increased. All inks have a low viscosity and are acceptable for inkjet printing.

Fig. 1 shows the variation of the formulated inks viscosities by increasing the shear rate on

a logarithmic scale. The viscosity of all samples remained constant with increasing shear rate. It is apparent that the constant changes in viscosity values by increasing the shear rates indicating the inks behave as the Newtonian fluid.

Table 5 shows the surface tension and contact angle of Ink 1 to Ink 9. Ink 1 to Ink 5, the contact angle and surface tension decrease with increasing oxygen groups in the structure of the glycol ethers used in the ink formulation. As shown in Table 2, with the increase of ethylene groups in glycol ethers, the dipole moment has increased from Ink 1 to Ink 5; consequently, the ink has become more polarized, and hydrophilicity increased, which improved wettability properties. Ink 9, which contains butyric acid as a complexing agent in its formulation, has the lowest contact angle value. Table 3 shows the structure of the complexing agents used in the ink formulations. The contact angle decreased by increasing the length of the alkyl chain of organic acid used in the ink formulation as the complexing agent, which is in line with the reported literature results [11,12].

It should be considered that the complexing agent role is improving the solubility of indium acetate in water. Butyric acid has the lowest contact angle of formulated inks as a complexing

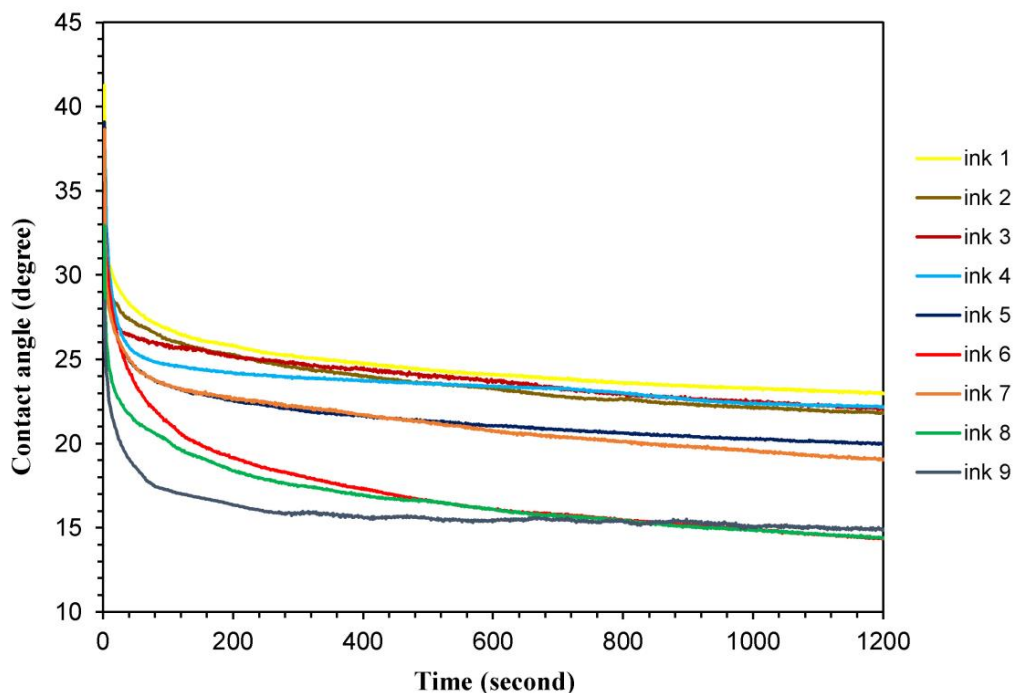


Fig. 2. Chart of contact angle of inks in terms of time (inks 1-9)

agent. Nevertheless, only acetic acid could dissolve indium acetate in water entirely, and other acids could not completely dissolve indium acetate (Table 6). Therefore, it could be concluded that acetic acid was selected as the best complexing agent for ink formulation.

Fig. 2 also shows the contact angle changes with time on the glass substrate. As can be seen in all the diagrams, it is evident that first, there was an initial decrease in the initial times, and then over time, the value of the contact angle first decreased slightly and then remained constant.

Initially, a decrease in the contact angle was observed due to the initial adsorption of the ink droplet by the glass substrate and its spreading on it, and then over time, the value of the contact angle remained almost constant.

In general, it could be concluded that Ink 5, which contains polyethylene glycol as co-solvent and acetic acid as a complexing agent, has the lowest contact angle and thus was selected as the best ink formulation. To ensure the obtained results, the contact angle measurements were

repeated for the formulated inks, and the obtained results were consistent with the previous results.

Thermogravimetric analysis

Fig. 3 shows the TG and DTG curves of the Ink 5 solution. It can be seen from the curves that an initial decrease in 50% weight loss occurred between room temperature to 120 °C due to evaporation of water and acetic acid used in the ink solution. The weight loss continued in the next step from 120 °C to 180 °C by decomposition of other organic components used in the ink formulation, such as glycol ether co-solvent. At last, another decrease in weight loss in the range of 180 °C to 330 °C observed, which indicates the oxidation of precursor ink of indium acetate and the formation of indium oxide in this temperature range [13]. TG/DTG curves were measured to determine the appropriate temperature for the oxidation, so in thermal treatment by applying the 350 °C temperature, the indium oxide nanoparticles crystallized and converted to oxide phase.

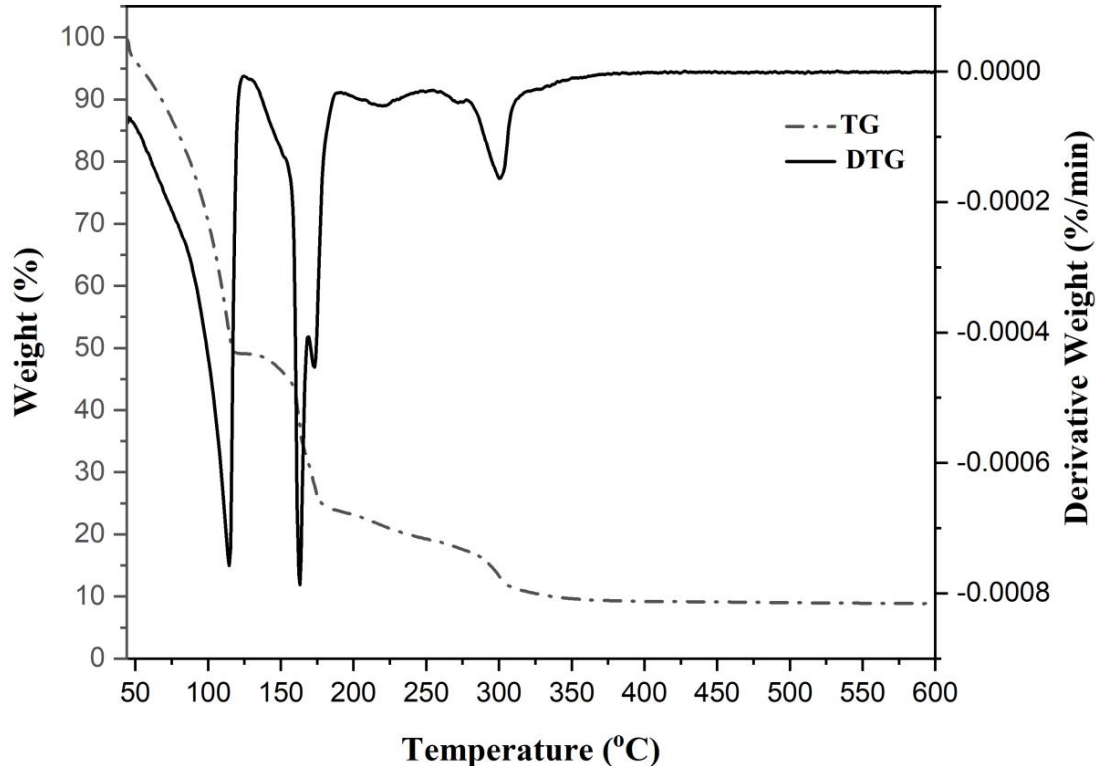


Fig. 3. TG/DTG curves of the solution of Ink 5

Surface treatment of the glass substrate

Surface treatment by plasma

One economical, cost-effective, and environmentally friendly method to improve the wettability of glass substrate is the plasma method. The purpose of surface modification by plasma is to create special functional groups that can react and change the free energy of the surface and ultimately improve the chemical adhesion of the printed layer to the surface. The interaction of plasma with the surface causes the removal of contaminants from the surface and causes ion and electron bombardment and tiny engravings on the surface that can not be created by physical abrasion [14,15]. This method, which involves cleaning the surface from dirt and roughening the surface, improves the surface's wettability.

The plasma process under oxygen gas is based on oxygen induction and leads to chemical groups, including hydroxyl and carboxyl. The created

functional groups play a critical role in creating polar groups and increasing the hydrophilicity of the glass surface [16]. The plasma under nitrogen gas also leads to forming amine functional groups. Nitrogen plasma generally improves wettability and adhesion properties [17].

Surface treatment by washing with Piranha solution

The Piranha solution is a mixture of sulfuric acid and hydrogen peroxide used as a robust oxidant solution. Piranha solution removes metals and organic contaminants and will improve the hydrophilicity of glass surfaces. It is prepared by first adding 30 ml of concentrated sulfuric acid to a beaker and then gently adding 30 ml of 30% hydrogen peroxide when stirring vigorously. Different sulfuric acid and hydrogen peroxide ratios can be used (3: 1 and 5: 1) [18].

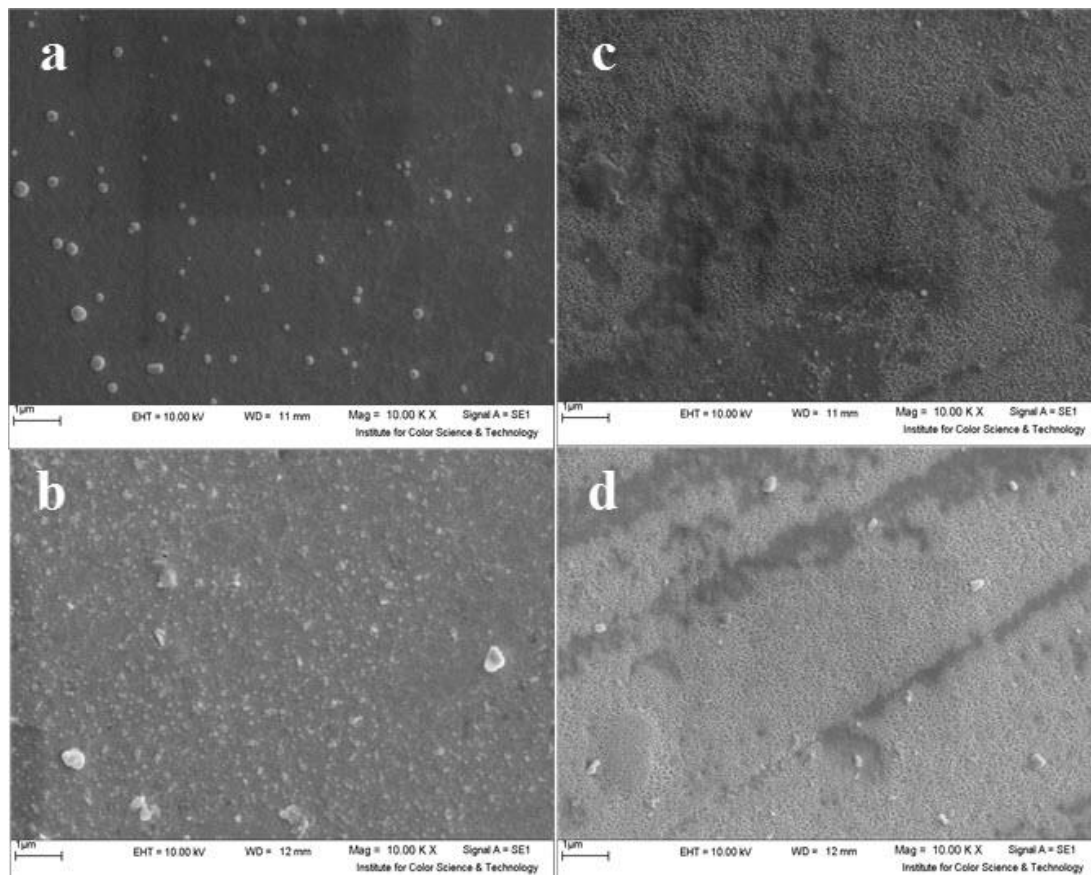


Fig. 4. SEM images of the surface of printed samples a) not treated glass substrate, b) piranha treated, c) O_2 plasma treated, d) N_2 plasma treated)

In this study, to remove possible contaminants and impurities from the glass substrate, glass slides were placed in piranha solution for 45 minutes, then immersed in deionized water for 5 minutes, and this step was repeated three times.

Washing glass substrates with piranha solution, an oxidizing agent, removes impurities and surface contaminants; makes the surface hydrophilic because the piranha solution hydroxylates the surface and adds OH functional groups to the surface [19].

SEM images of printed samples

Fig. 4 shows the SEM images of printed samples with the optimal ink formulation (Ink 5 containing polyethylene glycol as co-solvent and acetic acid as complexing agent) on the glass substrate, without any particular physical and chemical treatment,

piranha, cleaned glass substrate, and plasma-treated glass substrate.

SEM images show that ink based on indium acetate printed better and more uniformly on plasma glass surfaces under nitrogen gas. Plasma treatment under nitrogen has caused surface modification of the glass substrate and added amine functional groups to the glass substrate, thus increasing the wettability and hydrophilic properties.

Structural analysis of printed indium oxide thin film XRD analysis

XRD measurements investigated the crystal structure of IO thin film. The XRD patterns are illustrated in Fig. 5. All detected peaks could be indexed to body-centered cubic (bcc) IO (JCPDS card NO 06-0416). The sharp peaks revealed the

Table 7. Structural parameters (crystallite size and lattice constant) of the IO inkjet printed film

Film thickness (nm)	Crystallite size (nm)	Lattice constant (Å)
96.39	14.4	10.1769

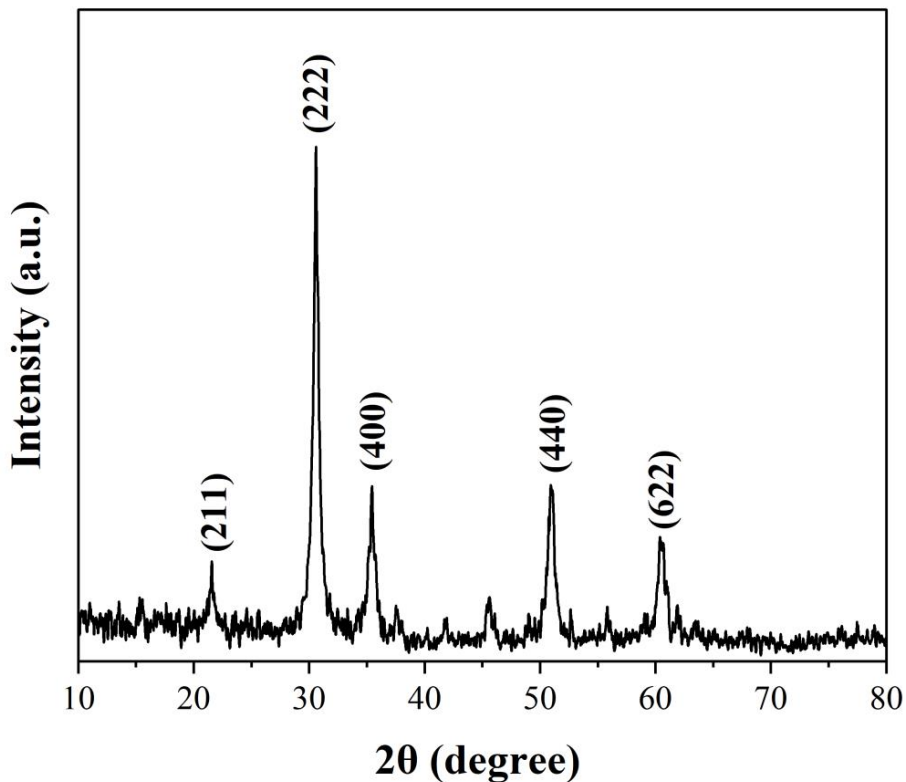


Fig. 5. The XRD patterns of IO thin film

crystallinity of the thin film and no impurity was identified. The crystallite size (D) was calculated by Debye–Scherrer formula (equation 1) along with (2 2 2) direction, which was the preferred growth orientation.

$$D = \frac{(0.9 \times \lambda)}{(\beta \cos \theta)} \quad (1)$$

Where λ is the X-ray wavelength ($\lambda = 1.5406 \text{ \AA}$), θ

is the diffraction angle, and β is the line broadening at half the maximum intensity full width (FWHM) in radians. Table 7 presents the crystallite size and the lattice constant of the IO inkjet printed film.

Morphological analysis of printed indium oxide thin film

FESEM analysis

Fig. 6 shows the FESEM image of IO thin film

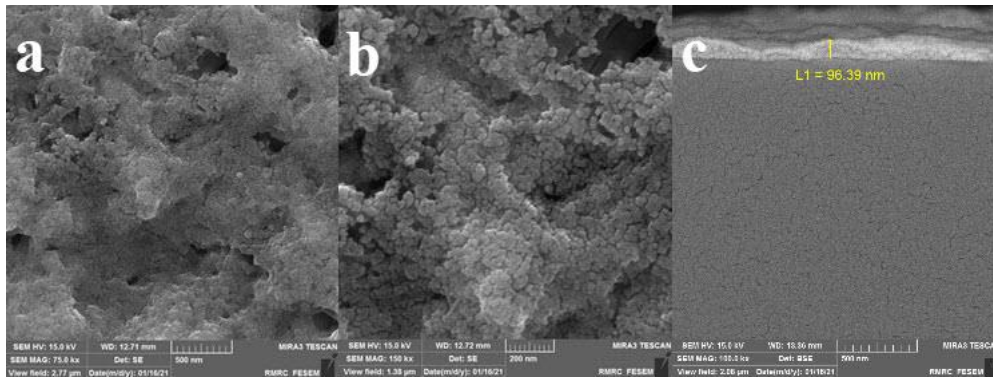


Fig. 6. a, b) FESEM images of the surface of the printed IO nano thin film, c) cross-section of the printed IO nano thin film fabricated by 3 print passes on the glass substrate

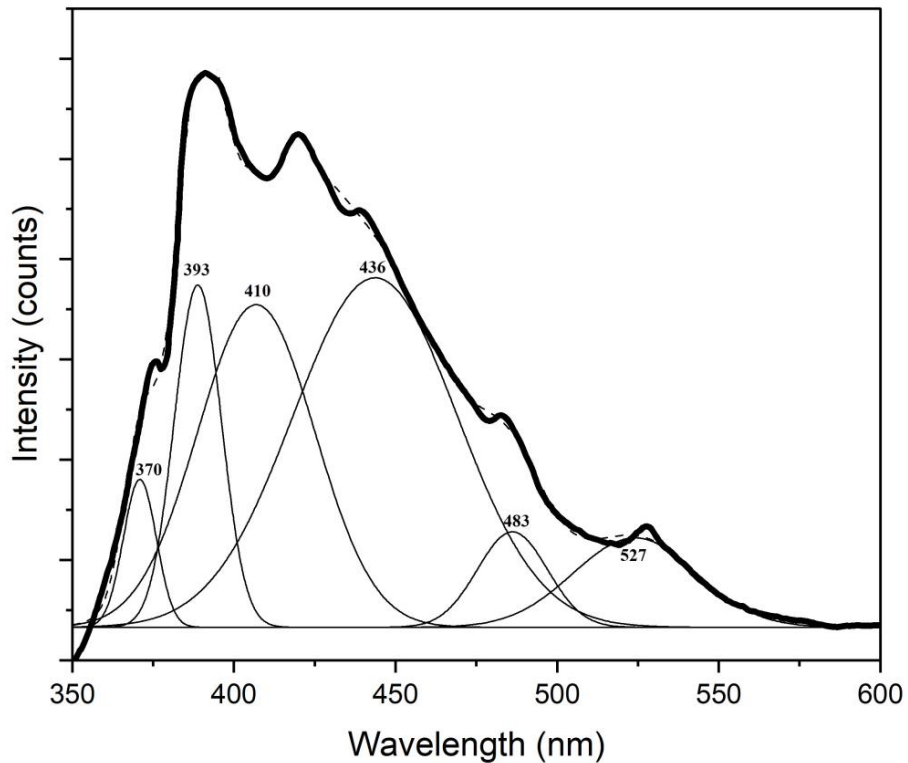


Fig. 7. Deconvolution of PL spectra for IO inkjet-printed thin film

after thermal treatment, revealing that IO thin film consists of crystalline nanoparticles, which are not agglomerated. The magnified FESEM image of IO thin film (Fig. 6, b) shows that most IO nanoparticles are spherical. IO thin film is uniform, and nanoparticles distribute homogeneously throughout the film. The film's surface exhibited polycrystalline nature with a grain size below 20 nm. The cross-sectional view of the IO nano thin film (Fig. 6c) indicated dense and uniform nano structure of printed film. The thickness of nano thin film fabricated by 3 print passes is 96.39 nm.

Photoluminescence analysis

PL spectrum is related to the materials' microstructure, electronic state, defect state, and energy level structure. It is known that bulk IO cannot emit light at room temperature; in contrast, nano-scaled IO films are reported to display PL response [20,21]. Fig. 7 shows that the PL spectrum of the IO thin film was measured at room temperature under an excitation wavelength of 320 nm. Deconvolution of PL spectra for IO thin film carried out by the method

of multi peaks gaussian fitting to detailed study of emissions through defects. The PL spectra comprised of 6 bands peaking at approximately 370,393,410,436,483 and 527 nm, respectively.

A strong emission peak was observed in the ultraviolet region centered at 393 nm. The reported Blue emission at 410 nm is due to the deep level emission of oxygen defects in the nanostructure of IO thin film[22,23]. The 436 nm band is possibly due to the defect of In–O vacancy [24]. PL peak at 483 nm was attributed to the formation of single ionized oxygen defects [25]. A weak green emission peak centered at 527 nm also originated from deep level defects such as surface defects and singly ionized oxygen vacancies [26]. In this research, oxygen vacancies would be generated due to the incomplete oxidation of precursor ink solution during the thermal treatment process.

Optical analysis

Fig. 8 shows the optical transmittance of printed IO thin film on the glass substrate. The high optical transmittance is a vital intrinsic property for TCE materials. The optical transmittance of IO thin film

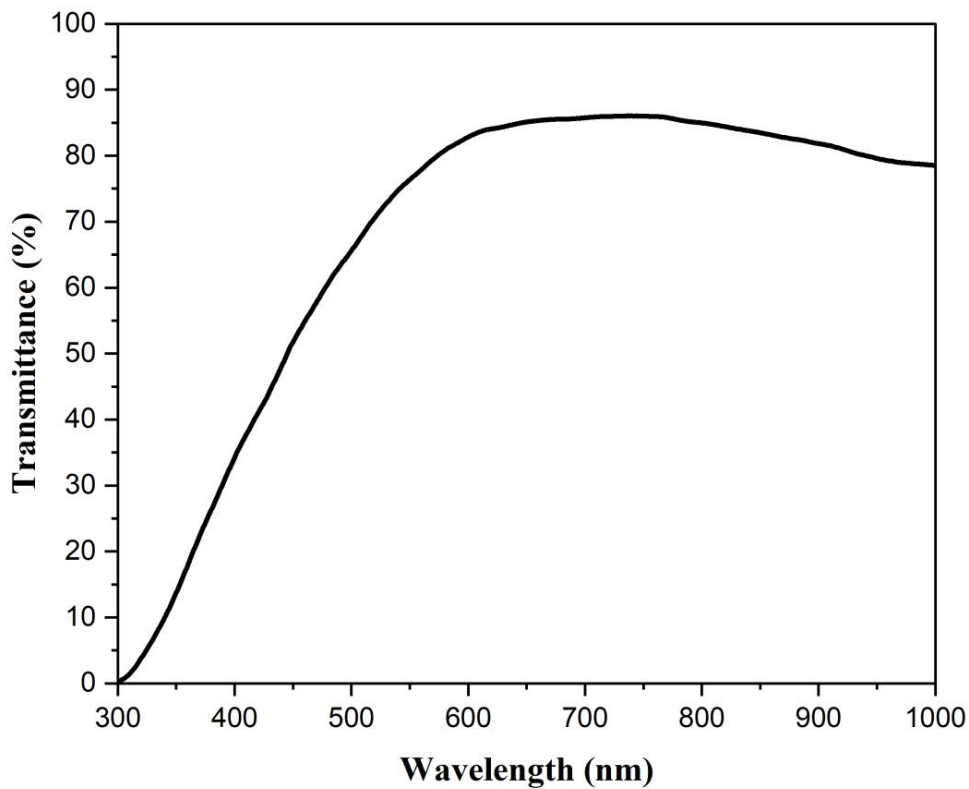


Fig. 8. Transmittance spectra of the IO inkjet-printed thin film

is above 82% at 550 nm.

Based on UV-Vis spectra, the optical band gap energy of IO thin film calculated by using Tauc's relation (equation 2) [27]:

$$\alpha h\nu = A(h\nu - E_g)^m \quad (2)$$

where α is the absorption coefficient, h is the Planck's constant, ν is the frequency of incident light, A is an energy independent constant, E_g is the optical band gap energy and m assumes values of 1/2 and 2 for allowed direct and allowed indirect electronic transitions, respectively. In this case, the band gap energy has been estimated by assuming an allowed direct transitions.

Fig. 9 illustrates the dependence of the absorption coefficient $(\alpha h\nu)^2$ against photon energy ($h\nu$) for IO thin film. By extrapolating the linear region of the curve to horizontal axis the band gap (E_g) of IO thin film determined 3.6 eV. Due to quantum confinement effect, the band

gap energy increases by decreasing crystallite size [28,29]. As in this work the IO thin film has the small size crystallite size, the band gap energy is higher than bulk indium oxide and comparable to the reported results [30–33].

Raman analysis

Fig. 10 shows Raman spectra of the IO thin film at room temperature in the frequency range of 100–700 cm^{-1} . The cubic structure of IO belongs to the space group I_a^3 and T_h^7 . IO has vibration modes for this structure with symmetry A_g , E_g , T_g (Raman active), and T_u (IR active) [34]. As seen in Fig. 8, the measured Raman spectra of IO thin film show peaks at 131, 307, 366, 495, 560, and 631 cm^{-1} . These values are in good agreement with those previously reported in the literature [35–38]. A wide peak centered at 560 cm^{-1} originated from the glass substrate [39]. As XRD results, the Raman spectra approved the cubic bixbyite crystal structure of nano IO thin film.

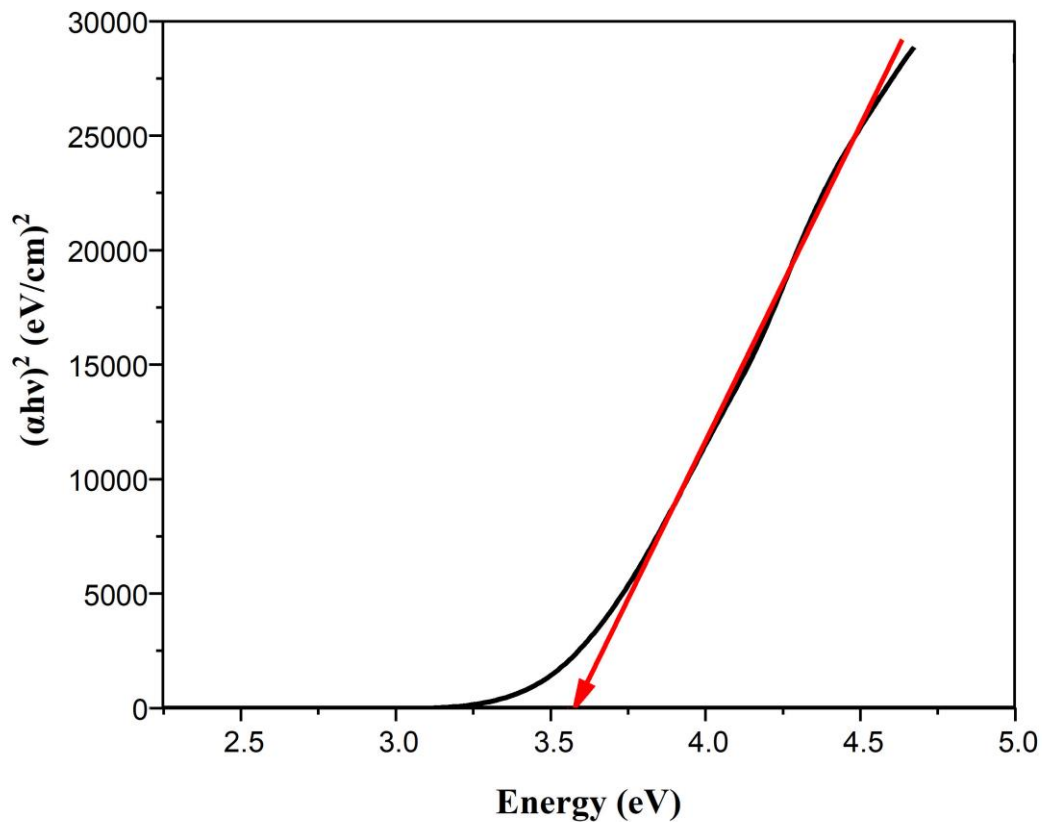


Fig. 9. Optical band gap energy (E_g) of the IO inkjet-printed thin film

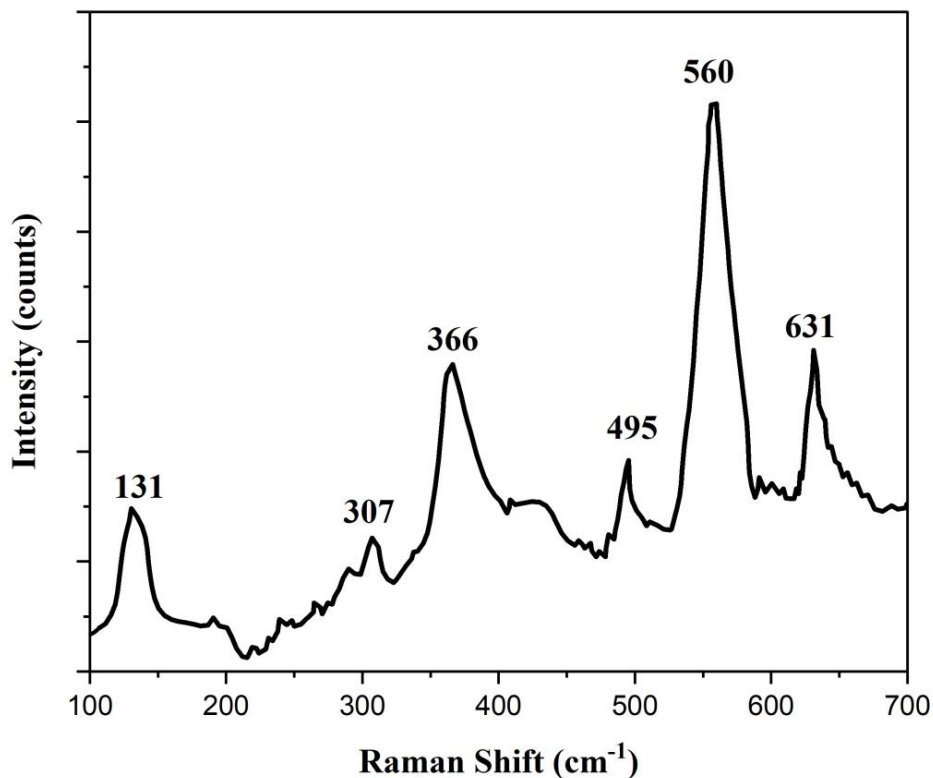


Fig. 10. Raman spectra of the IO inkjet-printed thin film

CONCLUSION

The IO nano thin film was fabricated on the glass substrate using an eco-friendly and cost-effective inkjet printing method. Various water-based indium acetate ink solutions differ in co-solvents and complexing agents formulated. Co-solvents were applied to tune indium acetate inks' viscosity and surface tension. Different methods also applied for substrate pretreatment, and plasma treatment was selected as an environmentally friendly and cost-effective method, which improved the substrate's wettability and enhanced the printed film's adhesion to prevent cracking during the thermal process.

After obtaining the optimum ink formulation (Ink 5), which supported rheological behavior and wettability properties, the indium acetate ink solution as precursor was deposited on the plasma treated glass substrate via inkjet printing and, consequently, thermal treatment was performed to produce dense and uniform IO nano thin film. Complete characterizations were utilized on the prepared IO film by different analyses such as XRD, FESEM, PL, and Raman, which approved the smooth and homogenous nanoscale layer.

ACKNOWLEDGEMENT

This work was done as a research project in Institute for Color Science and Technology, by financial support of INSF (Iran National Science Foundation).

CONFLICTS OF INTEREST

The authors declare that there is no conflict of interests regarding the publication of this manuscript.

REFERENCES

1. Transparent Conductive Materials: Wiley; 2018.
2. Crawford GP. Flexible Flat Panel Display Technology. Flexible Flat Panel Displays: Wiley; 2005. p. 1-9.
3. Chemical Solution Deposition of Functional Oxide Thin Films. Springer Vienna; 2013.
4. Krainer S, Smit C, Hirn U. The effect of viscosity and surface tension on inkjet printed picoliter dots. RSC Advances. 2019;9(54):31708-31719.
5. Bretos I, Jiménez R, Ricote J, Calzada ML. Low-temperature crystallization of solution-derived metal oxide thin films assisted by chemical processes. Chemical Society Reviews. 2018;47(2):291-308.
6. Grüßer M, Waugh DG, Lawrence J, Langer N, Scholz D. On the Droplet Size and Application of Wettability Analysis for the Development of Ink and Printing Substrates. Langmuir. 2019;35(38):12356-12365.

7. Arfsten NJ. Sol-gel derived transparent IR-reflecting ITO semiconductor coatings and future applications. *Journal of Non-Crystalline Solids*. 1984;63(1-2):243-249.
8. Soleimani-Gorgani A. Inkjet Printing. *Printing on Polymers*: Elsevier; 2016. p. 231-246.
9. Cummins G, Desmulliez MPY. Inkjet printing of conductive materials: a review. *Circuit World*. 2012;38(4):193-213.
10. Maleki H, Bertola V. Recent advances and prospects of inkjet printing in heterogeneous catalysis. *Catalysis Science and Technology*. 2020;10(10):3140-3159.
11. Bhattacharjee S, Khan S. Effect of alkyl chain length on the wetting behavior of imidazolium based ionic liquids: A molecular dynamics study. *Fluid Phase Equilib*. 2019;501:112253.
12. Blanco D, Viesca JL, Mallada MT, Ramajo B, González R, Battez AH. Wettability and corrosion of [NTf₂] anion-based ionic liquids on steel and PVD (TiN, CrN, ZrN) coatings. *Surface and Coatings Technology*. 2016;302:13-21.
13. Jain P, Su C, Haga K-i, Tokumitsu E. Electrical and patterning properties of direct nanoimprinted indium oxide (In_2O_3) and indium tin oxide (ITO). *Japanese Journal of Applied Physics*. 2019;58(SD):SDDJ05.
14. Terpilowski K, Rymuszka D. Surface properties of glass plates activated by air, oxygen, nitrogen and argon plasma. *Glass Phys Chem*. 2016;42(6):535-541.
15. Vázquez Manzano F, Rodríguez Suárez, Luísa P. y García Landa, José A. (2017). Corporalidad, Temporalidad, Afectividad. *Perspectivas filosófico-antropológicas*. Logos Verlag Berlin GmbH. Berlín. *Differenz*. 2018(4):111-117.
16. Li D, Xiong M, Wang S, Chen X, Wang S, Zeng Q. Effects of low-temperature plasma treatment on wettability of glass surface: Molecular dynamic simulation and experimental study. *Applied Surface Science*. 2020;503:144257.
17. Iwasaki M, Matsuda Y, Takeda K, Ito M, Miyamoto E, Yara T, et al. Roles of oxidizing species in a nonequilibrium atmospheric-pressure pulsed remote O_2/N_2 plasma glass cleaning process. *Journal of Applied Physics*. 2008;103(2).
18. Bhalla V, Carrara S, Stagni C, Samorì B. Chip cleaning and regeneration for electrochemical sensor arrays. *Thin Solid Films*. 2010;518(12):3360-3366.
19. Zhang R, Liao W, Sun Y, Heng JYY, Yang Z. Investigating the Role of Glass and Quartz Substrates on the Formation of Interfacial Droplets. *The Journal of Physical Chemistry C*. 2018;123(2):1151-1159.
20. Wu P, Li Q, Zhao CX, Zhang DL, Chi LF, Xiao T. Synthesis and photoluminescence property of indium oxide nanowires. *Applied Surface Science*. 2008;255(5):3201-3204.
21. Liang CH, Meng GW, Lei Y, Philipp F, Zhang LD. Catalytic Growth of Semiconducting In_2O_3 Nanofibers. *Adv Mater*. 2001;13(17):1330.
22. Anand K, Kaur J, Singh RC, Thangaraj R. Structural, optical and gas sensing properties of pure and Mn-doped In_2O_3 nanoparticles. *Ceram Int*. 2016;42(9):10957-10966.
23. Gan J, Lu X, Wu J, Xie S, Zhai T, Yu M, et al. Oxygen vacancies promoting photoelectrochemical performance of In_2O_3 nanocubes. *Sci Rep*. 2013;3(1).
24. Kundu S, Biswas PK. Synthesis and photoluminescence property of nanostructured sol-gel indium tin oxide film on glass. *Chemical Physics Letters*. 2005;414(1-3):107-110.
25. Najwa S, Shuhaimi A, Talik NA, Ameera N, Sobri M, Rusop M. In-situ tuning of Sn doped In_2O_3 (ITO) films properties by controlling deposition Argon/Oxygen flow. *Applied Surface Science*. 2019;479:1220-1225.
26. Yadav K, Mehta BR, Singh JP. Template-free synthesis of vertically aligned crystalline indium oxide nanotube arrays by pulsed argon flow in a tube-in-tube chemical vapor deposition system. *J Mater Chem C*. 2014;2(31):6362-6369.
27. Tauc J. *Optical Properties of Amorphous Semiconductors*. Amorphous and Liquid Semiconductors: Springer US; 1974. p. 159-220.
28. Kelgenbaeva Z, Khandaker JI, Ihara H, Omurzak E, Sulaimankulova S, Mashimo T. Thermal and Optical Properties of In and In_2O_3 Nanoparticles Synthesized Using Pulsed Plasma in Water. *physica status solidi (a)*. 2018;215(11).
29. Wang YG, Lau SP, Lee HW, Yu SF, Tay BK, Zhang XH, et al. Photoluminescence study of ZnO films prepared by thermal oxidation of Zn metallic films in air. *Journal of Applied Physics*. 2003;94(1):354-358.
30. Dasari SG, Nagaraju P, Yelsani V, Tirumala S, M V RR. Nanostructured Indium Oxide Thin Films as a Room Temperature Toluene Sensor. *ACS Omega*. 2021;6(27):17442-17454.
31. Yahia A, Attaf A, Saidi H, Dahnoun M, Khelifi C, Bouhdjer A, et al. Structural, optical, morphological and electrical properties of indium oxide thin films prepared by sol gel spin coating process. *Surfaces and Interfaces*. 2019;14:158-165.
32. Bierwagen O. Indium oxide—a transparent, wide-band gap semiconductor for (opto)electronic applications. *Semicond Sci Technol*. 2015;30(2):024001.
33. Shaalan NM, Rashad M, Abdel-Rahim MA. Repeatability of indium oxide gas sensors for detecting methane at low temperature. *Mater Sci Semicond Process*. 2016;56:260-264.
34. Berengue OM, Rodrigues AD, Dalmaschio CJ, Lanfredi AJC, Leite ER, Chiquito AJ. Structural characterization of indium oxide nanostructures: a Raman analysis. *J Phys D: Appl Phys*. 2010;43(4):045401.
35. Kranert C, Schmidt-Grund R, Grundmann M. Raman active phonon modes of cubic In_2O_3 . *physica status solidi (RRL) – Rapid Research Letters*. 2014;8(6):554-559.
36. Lee H, Kim B, Gao CY, Choi HJ, Ko J-H, Seo CH, et al. Raman spectroscopy study of solution-processed In_2O_3 thin films: effect of annealing temperature on the characteristics of In_2O_3 semiconductors and thin-film transistors. *Molecular Crystals and Liquid Crystals*. 2019;679(1):38-47.
37. Liu D, Lei WW, Zou B, Yu SD, Hao J, Wang K, et al. High-pressure x-ray diffraction and Raman spectra study of indium oxide. *Journal of Applied Physics*. 2008;104(8).
38. Arooj S, Xu T, Hou X, Wang Y, Tong J, Chu R, et al. Green emission of indium oxide via hydrogen treatment. *RSC Advances*. 2018;8(21):11828-11833.
39. Chandrasekhar R, Choy KL. Innovative and cost-effective synthesis of indium tin oxide films. *Thin Solid Films*. 2001;398-399:59-64.